
Masters Theses

Student Theses and Dissertations

Spring 2019

Gel composition and brine concentration effect on hydrogel dehydration subjected to uniaxial compression

Xinrui Zhao

Follow this and additional works at: https://scholarsmine.mst.edu/masters_theses



Part of the [Petroleum Engineering Commons](#)

Department:

Recommended Citation

Zhao, Xinrui, "Gel composition and brine concentration effect on hydrogel dehydration subjected to uniaxial compression" (2019). *Masters Theses*. 7899.

https://scholarsmine.mst.edu/masters_theses/7899

This thesis is brought to you by Scholars' Mine, a service of the Missouri S&T Library and Learning Resources. This work is protected by U. S. Copyright Law. Unauthorized use including reproduction for redistribution requires the permission of the copyright holder. For more information, please contact scholarsmine@mst.edu.

GEL COMPOSITION AND BRINE CONCENTRATION EFFECT ON HYDROGEL
DEHYDRATION SUBJECTED TO UNIAXIAL COMPRESSION

by

XINRUI ZHAO

A THESIS

Presented to the Faculty of the Graduate School of the
MISSOURI UNIVERSITY OF SCIENCE AND TECHNOLOGY

In Partial Fulfillment of the Requirements for the Degree

MASTER OF SCIENCE

in

PETROLEUM ENGINEERING

2019

Approved by

Dr. Baojun Bai, Advisor

Dr. Shari Dunn Norman

Dr. Mingzhen Wei

© 2019

XINRUI ZHAO

All Rights Reserve

ABSTRACT

Gel treatment is a process that injects the gel into a reservoir to control the conformance and improve the sweep efficiency of injection fluids. At a certain pressure gradient, the gel dehydrates in a reservoir due to mechanical forces. This work evaluates the effects of the gel composition and brine concentration on gel dehydration under uniaxial compression. A sodium acrylate-co-acrylamide based gel cross-linked with N, N'-Methylenebisacrylamide (MBAA) was used for the study. The compression test is performed with a rheometer with a plate-plate geometry. The gel dehydration under pressure was measured to see how gel dehydration would be impacted by the brine concentration or the change in gel compositions including monomer and crosslinker concentration. Then, the elastic modulus (G') and the loss modulus (G'') of the gels before and after the compression were measured. This process aimed to assess the variations of the gel mechanical properties caused by compression-induced dehydration. The result shows the gel composition has a great impact on the gel dehydration under uni-axial compression. The amount of gel dehydration increases when gel swelling degree increases for all experimental factors. The gel after compression has a lower G' and a higher G'' compared with the gel before compression, indicating damage on gel networks. This work is of significance on optimizing gel treatments for conformance control. It may also provide a reference for hydrogel applications in other fields.

ACKNOWLEDGMENTS

I would like to express my deep appreciation and gratitude to my advisor, Dr. Baojun Bai for his patient guidance and mentorship. Dr. Bai shows me how to be an outstanding research scientist in terms of skills in critical thinking, writing, speaking, and teaching. Moreover, I also learned what a perfect work should be and the spirit of working hard and carefulness, which will benefit my future career.

I also appreciate the help of my lab group. I would like to express my deep gratitude to Xindi Sun, Yifu Long, Jiaming Geng, Jingyang Pu, Ze Wang, Ali, Enze Zhou, Bowen Yu, and Haifeng Ding for their help and teamwork.

The work is partially supported by the grant from the US Department of Energy under contract of DE-FE0024558.

Special thanks to my family for their support and encouragement. I would also like to express my deep love for my family and significant others for their great support and care.

TABLE OF CONTENTS

	Page
ABSTRACT.....	iii
ACKNOWLEDGMENTS	iv
LIST OF ILLUSTRATIONS.....	vii
LIST OF TABLES.....	ix
 SECTION	
1. INTRODUCTION	1
2. LITERATURE REVIEW	4
2.1. HYDROGEL USED FOR CONFORMANCE CONTROL	4
2.2. GEL DEHYDRATION IN RESERVOIR CONDITION	5
2.3. COMPRESSION-INDUCED GEL DEHYDRATION.....	6
2.4. THE INFLUENCE OF COMPRESSION VELOCITY ON STRENGTH AND STRUCTURE FOR GELLAN GELS.....	8
2.5. SOLVENT RELEASE FROM HIGHLY SWOLLEN GELS UNDER COMPRESSION.....	10
2.6. COMPRESSIBLE BEHAVIORS OF GELLAN HYDROGELS IN A CONSTRAINED GEOMETRY AT ULTRASLOW STRAIN RATES	14
2.7. VARIABLE MESO-MODEL FOR MECHANICAL AND WATER EXPULSED BEHAVIORS OF PVA HYDROGELS UNDER COMPRESSION	20
3. EXPERIMENTAL STUDIES	26
3.1. MATERIALS & SYNTHESIS	26
3.1.1. Chemicals.....	26
3.1.2. Gel Disk Preparation.....	26

3.2. METHOD.....	28
3.2.1. Swelling Degree Measurement.....	28
3.2.2. Compression Test.	30
3.2.3. Measurement of Storage Modulus and Loss Modulus.	34
4. EXPERIMENTAL STUDIES	35
4.1. EFFECT OF BRINE CONCENTRATION	35
4.2. EFFECT OF CROSSLINKER CONCENTRATION	41
4.3. EFFECT OF MONOMER CONCENTRATION	45
5. CONCLUSIONS.....	49
REFERENCES	50
VITA.....	53

LIST OF ILLUSTRATIONS

	Page
Figure 2.1 Gellan gels' fracture behavior at different strain rates.	8
Figure 2.2 Presentation of water releasing from compressed gel disk (concave shape) and gel with no solvent release.	11
Figure 2.3 Gel deformation as a function of pressure for gels with a swelling ratio of 140 g/g (1), 100 g/g (2), 60 g/g (3), and 20 g/g (4).	12
Figure 2.4 Change in the volume of the gel as a function of the pressure of potassium Gels of different initial volumes.	14
Figure 2.5 Two geometries C1 and C2 with different boundary conditions employed in compression measurements.	16
Figure 2.6 Stress-strain curves of the gellan gels compressed at various crosshead speeds under C1 and C2 conditions.	17
Figure 2.7 Presentation of the gel sample before the compression.	18
Figure 2.8 Volume variation of gellan gels during compression at various crosshead speeds under C1 and C2 conditions.	19
Figure 2.9 The crack pattern of gels in C1 condition under compressions and that of the gels in C2 condition under ultraslow compressions.	20
Figure 2.10 (a) A PVA gel sample; (b) A micro view of a sample with confocal laser scanning microscopy.	21
Figure 2.11 The uniaxial static compression test with the electromagnetic dynamic mechanical test system.	22
Figure 2.12 The schematic diagram of a fiber frame.	23
Figure 2.13 Model is constructed by three parts: free water (green), bound water (blue) and fiber (yellow). ...	25
Figure 3.1 Gelation in the test tube.	28
Figure 3.2 Presentation of the gel disk in a fully swollen state and gel in the dry state ...	29
Figure 3.3 The gel disk placed between the upper and lower plates.	30

Figure 3.4 The concave shape of the compressed gel disk	32
Figure 3.5 Glass chip with a larger diameter used during the compression test.....	33
Figure 4.1 Volume loss as a function of the pressure for gels swollen in different brines	39
Figure 4.2 Change in storage modulus (G') and loss modulus (G'') for gels swollen in different brines	40
Figure 4.3 Volume loss as a function of pressure for gels with different initial crosslinker concentrations	43
Figure 4.4 Change in storage modulus (G') and loss modulus (G'') for gels with different crosslinker concentrations	44
Figure 4.5 Volume loss as a function of pressure for gels with different initial monomer concentration.	47
Figure 4.6 Change in storage modulus (G') and loss modulus (G'') for gels with different initial monomer concentration.....	48

LIST OF TABLES

	Page
Table 3.1 Gel samples with different gel formulation.	27
Table 4.1 The swelling ratio of gels swollen in different brines	36
Table 4.2 The swelling ratio of the gel with different initial crosslinker concentration...	41
Table 4.3 Swelling ratio of gels with different initial monomer concentration.....	46

1. INTRODUCTION

Hydrogels are chemically cross-linked charged polymer networks that can swell in aqueous solutions up to several hundred times. It also has a striking ability to keep their shape even when polymer concentration is low. Owing to these unique properties, hydrogels are widely applied in heterogeneous reservoirs with fractures or channels for conformance-control. For a conventional gel treatment, a gelant is injected into the reservoir as a liquid phase. Gelation takes place when the block agent is placed, correcting in-depth permeability of the reservoir. This in-situ gelation system has drawbacks including lack of gelation-time control, damage to the porous media, degradation, and dilution by formation water. In recent years, the preformed gel has been developed and applied to control the conformance. The preformed gel is formed at a surface facility before injection into the reservoir and thus able to overcome some of the shortages peculiar to the in-situ gelation system. Besides, recent works have shown that the nano-sized hydrogel has the potential to alter the wettability of reservoir rocks, therefore enhancing oil recovery (Geng et al., 2018 and Wang et al., 2018).

During gel placements, at a certain pressure gradient, gels lose water into porous media and are concentrated. In this case, the gel dehydration may be desirable since concentrated gels are less likely to washout (Seright, 1999). Gels continue dehydrating when displacing fluid (e.g. Water and gas) is injected. In contrast, gel dehydration at this stage reduces the plugging efficiency, leading to low sweep efficiency of the displacing fluid. Seright (1999, 2001, and 2003) investigated the gel dehydration during extrusion or propagation for both preformed gel and in-situ gels using fractured cores. Note that gel

dehydration varies the injection rate and time. In a study concerning the transportation of preformed particle gel (PPG) through open fractures, it is found that the particle gel dehydrates during the transportation and the plugging efficiency thus seriously reduces (Zhang et al., 2010). However, it is hard to evaluate the gel behavior when the experiment is carried out in the core. Toward a better understanding of the mechanisms of the gel dehydration, further investigations are needed.

During the last decades, hydrogel mechanical properties have been intensively studied. In some publications dealing with gel deformations, it is known that the classical elasticity theory can no longer be applied to hydrogels prepared in the presence of a solvent. In few rheological and/or compression experiments, if it is not placed in a bath of solvent, a gel releases solvent under simple shear or uniaxial compression (Zanina et al., 2002; Vervoort et al., 2005). Given the importance of the mechanical gel dehydration, however, only a few experimental investigations have been made on it as a function of uniaxial compression. Vervoort et al. (2005) demonstrate that the quantity of released water increases with pressure. A theoretical prediction of the volume loss of a weakly charged polyelectrolyte gel is given, showing that the gel with more charges per chain would also have the higher volume loss at a given value of the applied pressure. Urayama et al. (2008) indicate the reduction of the gel volume induced by the uniaxial compression could be more than 50% of its original volume. A slow compression measurement is conducted at a considerably low compression speed (0.005 mm/min), in which the gel is less easily to be fractured or crashed. Urayama et al. (2012) demonstrate the static and dynamic aspects of the volume change phenomena caused by constant uniaxial strain (either compression or stretching). In most publications dealing with compression-induced gel dehydration,

experiments were performed on two types of gels that have totally different monomer compositions for comparison. These experiments only considered limited affecting factors (for example, gel types and swelling degree) and aimed to observe and prove the occurrence of the gel dehydration.

The question discussed here is as follows: how would the gel dehydration be impacted by the change in the gel composition or the concentration of the brine used to swell the gel? On the basis of those publications mentioned in the last section, a compression test performed on fully swollen acrylamide (AM)/sodium acrylate (AA-Na) co-polymer gels were carried out in our lab. This test aimed to study the influences of crosslinker concentration, monomer concentration, and solvent type to the gel dehydration under uniaxial compression, respectively. The major challenge during the compression test is to evaluate the dehydration because the released water is extremely hard to measure. To address this problem, the released water is measured by monitoring the reduction in gel volume. The quantity of the water released from the gel is interpreted as a function of the pressure. The G' and G'' of the gel before and after the compression is measured. The effect of the change in gel composition and brine concentration to gel mechanical properties has been also discussed

2. LITERATURE REVIEW

2.1. HYDROGEL USED FOR CONFORMANCE CONTROL

Water production in oil production wells is a serious problem as the wells mature. In present, the average daily water production from oil wells is roughly 3 BWPD per barrel of oil. Operating cost is increased to lift and dispose of the produced water. For a well with a water cut of more than 80 %, the cost of treating water can double the normal lifting cost. Conformance control is one of the water control technology that intends to reduce water production and the costs of producing water.

Hydrogel has been used in conformance application in many years and gel treatments are most effective in reservoirs with fractures and severe channeling problems. Gels currently used for conformance control can be divided into two categories, according to the gelation methods. In-situ gel system is a technology in which the gelant is injected into the formation and the gel is formed under reservoir condition after the placement. In another word, the gelation occurs in the reservoir. In the past few decades, Chromium (3+) crosslinked polyacrylamide or its derivatives have been most widely used (Reddy and Reddy 2003). In a gel treatment, the gelant propagates through the fractures or channels, forming gels along the fracture to reduce channeling (Seright 1995). Since the gel is initially injected as a liquid phase, the gelant may leak off into the rocks and reduce productivity and oil-recovery efficiency. Another problem while using in-situ gel is the adsorption. During the transportation of the gelant, the component and the concentration of the solution may change as a result of the adsorption problems.

Preformed gels are gels formed in surface facilities before injection. Preformed gels that can swell up to 200 times are used as a novel fluid-diverting agent to overcome some shortages of the in-situ gelation system mentioned above. It has been proved that PPG for conformance control is efficient and cost-effective. Seright, Seldal et al. (1997), Seright (1999) studies the performance of the preformed bulk gel in fractured systems and the results demonstrate that the gel can efficiently plug the fractures. It is also found that the preformed bulk gel has better placement compared with in-situ gel and reduces the damage to low permeability zones in the reservoir (Seright 2003). Chauveteau, Omari et al. (2000) develops a microgel by polymer crosslinking under shear that can be used as a permeability modifier. Feng, Tabary et al. (2003) proves that the microgels can fluently transport through the porous media without forming any plugging, indicating these microgels have the potential for water-shutoff operation. Zhang, Challa et al. (2010), Bai and Zhang (2011) study the transportation of the PPG through porous media. It is found that the PPG propagation is like a piston along the fracture and PPG can reduce the permeability of the fracture by forming a gel pack after the placement in the fracture.

2.2. GEL DEHYDRATION IN RESERVOIR CONDITION

Gel dehydration is a serious problem that could compromise the efficiency of the gel treatment. At a pressure gradient, gel dehydration may occur, expelling some water out of the gel structure (Nguyen, Green et al. 2004). It concentrates the gel, and thus compromises the permeability reduction in fractures. The gel plugging efficiency is therefore decreased. Seright (1998) demonstrates that gel dehydration occurs during the extrusion through fractures, inducing a low rate of gel propagation. Nguyen, Green et al.

(2004) illustrates that the gel dehydration is affected by gel composition and applied pressure gradient. Brattekkås, Ersland et al. (2018) states that the dehydration of the gel is dependent on the gel properties, fracture properties, and the adjacent porous media. During the propagation, gel dehydration is a complex process, because it is controlled by both shear and compression. To understand the mechanism of the dehydration, we may investigate these two effects individually.

2.3. COMPRESSION-INDUCED GEL DEHYDRATION

The mechanical behavior of the hydrogel has been intensively studied by the researchers since 1950s, for example, hydrogels in uniaxial deformation, hydrogels under shear and their static or dynamic swelling properties. It is well recognized that the solvent releases from the hydrogel when subjected to shear. In contrast, in the past decades, most of the people believed that there is no solvent released from the hydrogel when the hydrogel is compressed. The gel under uni-axial compression can be interpreted by the classical network-elastic theory or using a scaling approach.

There are two ways of performing compression experiments that have been commonly used. The first one, where the gel is placed in a solvent bath, allows the solvent molecules inside and outside of the gel to easily exchange. However, this method has an inherent shortage that it is inaccessible to observe the solvent release from the gel because the gel is always in an equilibrium state. The second one generates when the gel is in the air. This process also has a limitation as a result of the evaporation of the solvent inside the gel. Depending on the gel types, the rate of water evaporation from gels can vary from 1.1×10^{-3} mg/s to 6×10^{-3} mg/s. (Vervoort, Patlazhan et al. 2005). Thus, the compression

experiments performed in the open air should be conducted in a relatively short time period to minimize the evaporation.

Recently, researchers have focused on solvent release from hydrogel under compression on account of its effects on hydrogel applications in many aspects. Hydrogels release solvent due to compression can be either favorable or disadvantageous depending on the type of the applications. Pills release drug component before transporting to the target organ can reduce the efficacy or even lead to an adverse reaction. Diapers when being used is routinely subjected to compression due to the human motions. Thus whether the diaper can maintain the absorbing ability under compression is a decisive factor for evaluating the products. During daily activities, the synovial joint is routinely subjected to static and dynamic loads. Though moderate activity is essential to maintain a functional tissue, joint overloading results in degradation of cartilage to a mechanically inferior tissue. Using hydrogel products to engineer man-made cartilage encounters gel dehydration under dynamic loads. The dehydration of the preformed particle gels used to plug the high-permeability zones resulting in a reduction of the plugging efficiency. Losing plugging efficiency may cause the failure of the project and therefore decrease the oil recovery and the economic benefit. In contrast, for some applications such as skin care that requires to release active components under mechanical stresses, this effect is positive. Investigations on compression-induced hydrogel volume loss challenged the old theories and interpretations, and help to improve the products.

2.4 THE INFLUENCE OF COMPRESSION VELOCITY ON STRENGTH AND STRUCTURE FOR GELLAN GELS

Nakamura, Shinoda et al. (2001) observes the solvent release from the hydrogel under compression in a study that investigates the influence of compression velocity on strength and structure for gellan gels. The gel samples used for compression measurements have a diameter of 5.75 mm and a height of 10 mm. The compression measurement is carried out using a commercial apparatus (Mini 55, Instron, USA) at different compression velocity changed from 1000 to 0.005 mm/min. To minimize the effect of the evaporation, the disks are covered with a commercial wrapping film for foods when the compression speed is low.

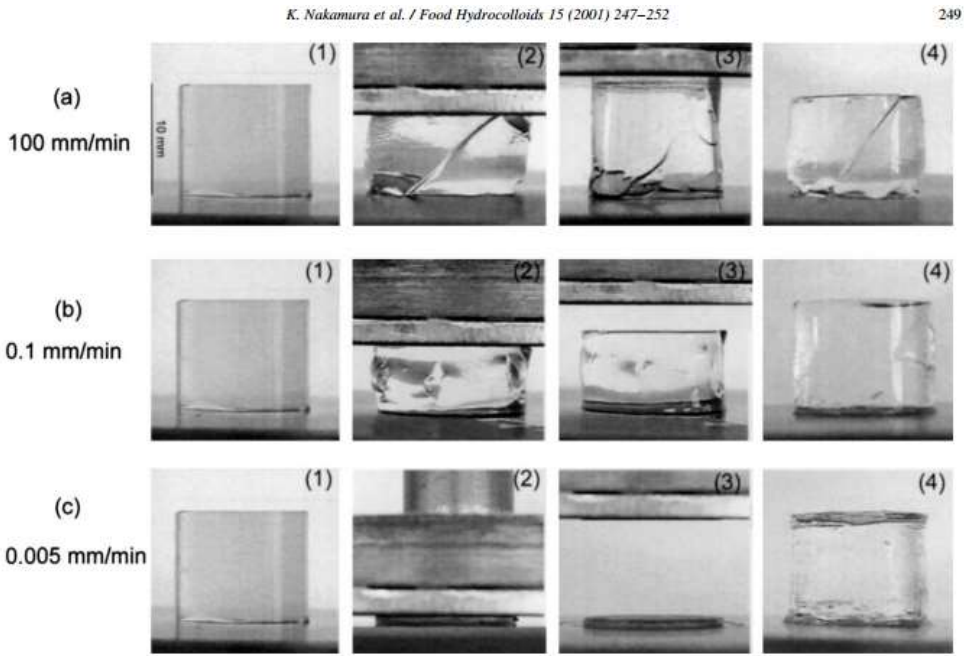


Figure 2.1 Gellan gels' fracture behavior at different strain rates. (Nakamura et al., 2001)

In this study, the gel sample under a compression rate of 100 mm/min breaks at a very small strain value (a). The gel is broken with a sharp break which intersects the whole gel disk at an angle of almost 45°. At a lower compression rate (b), the authors also observe some vertical fractures around the cylindrical surface. However, the sizes of the fractures are much smaller compared with those of the fractures shown in (a). Besides, they also notice that some water dropped down to the lower plate. Because the water on the surface is wiped out before the compression experiments, this water is considered as expelled water from the gel due to the gel deformation. At an extremely low compression speed of 0.0005 mm/min (c), the gel does not show any macroscopic fractures. Water is squeezed out of the gel incrementally with increasing compression.

After the compression experiments, these deformed gel samples are placed in the solvent again to absorb the solvent. It is found that the gel samples almost recover their initial volumes and shapes after reaching an equilibrium state. These results indicate that the gel can reswell to its original volume even the gel is compressed until one-tenth of its initial height. Another phenomenon worth taking note of is the difference on the surface of the gel samples. Gels undergo small deformations (a and b) show smooth surfaces after reswelling, while the gel deforms more than 90% (c) shows a rough surface. The authors illustrate that these damages on the surface are caused by the flow of the water. Because the compression is generated vertically, the water should flow radially. However, the roughness is also found on the top and bottom surface of the gel sample, which indicates the water inside the gel can flow both vertically and radially.

In most of the publications studying the gel mechanical behavior under compression, the result is only meaningful before the gel is cracked or fractured. In this

paper, the authors not only observe the gel dehydration under compression but also study the influence of the compression velocity on the gel structure, providing a reference for the experimental design of the gel compression experiments.

2.5 SOLVENT RELEASE FROM HIGHLY SWOLLEN GELS UNDER COMPRESSION

Vervoort, Patlazhan et al. (2005) notes that the solvent release from highly swollen gels under compression. They experimentally study the behavior of a strongly charged polyelectrolyte gel under uniaxial compression, demonstrating gel deformation and solvent loss at the same time. They also develop a theoretical interpretation for weakly charged gels based on a thermodynamic approach. In this study, the two types of polyelectrolyte gels used for this experiment are potassium acrylate-co-acrylamide gels with a swelling degree of 140-150 g/g and sodium acrylate-co-acrylic acid gels with a swelling degree of 200 g/g. Gels samples are swollen in distilled water until reaching an equilibrium state and are cut into disks for the compression experiments. The compression experiments are performed with an RMS-800 rheometer manufactured by Rheometrics. A gel disk is placed on the lower plate, the upper plate moves vertically at a constant speed to generate the uniaxial compression. The changes in the gel disk diameter measured at sample half-height are recorded using a CCD camera. The changes in gel disk height were recorded by the rheometer itself. During compression, to simplify the calculation, the sample volume is calculated as a cylinder volume with the diameter measured at a half height of the gel disk. It should be noticed that the experiments stop at the point when the deformation leads to gel breakage.

During compression experiments, gel disks of any swelling degree undergo solvent losses. The released water can be easily noticed on the lower plate when the gap is opened and the gel disk is removed. Another visual proof of the water expulsion is a concave shape of the gel disk during the compression shown in Figure 2.2. Because of the friction between the gel and the plate, the gel should be in a convex shape. But due to the expelled water near the upper and lower plate, the apparent sample shape becomes concave. The authors also note that no threshold pressure value for releasing water. The gel released the water as soon as the compression is performed and the gel disk is under load. During the compression experiments, once the compression is generated, a decrease in the normal force is detected, which indicates the gel volume loss.

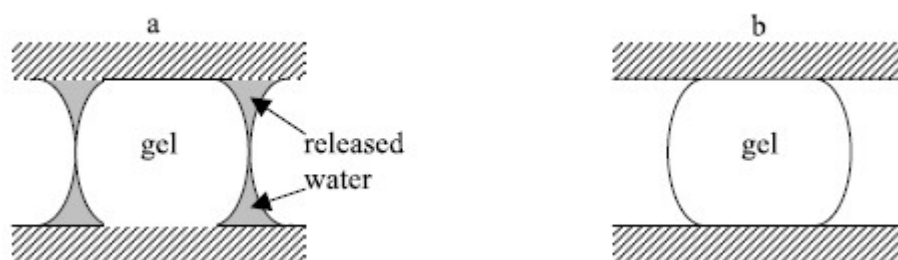


Figure 2.2 Presentation of (a) water releasing from compressed gel disk (concave shape) and (b) gel with no solvent release. (Vervoot et al., 2005)

In addition, the gel deformation as a function of pressure is discussed. As seen in Figure 2.3, the deformation-pressure curves for both potassium and sodium gels show an “s-shape”. The D/D_0 values are very low at the beginning of the compression is because the water releases from the gel and the normal force are low. In another word, at the beginning of the compression, the decrease in the gel height is mainly caused by the volume

loss instead of the radial stretching. This is shown in the inset (b) in Figure 2.3, in which the D/D_0 vs H/H_0 relation shows in-conformance with the dependence calculated for the case of volume conservation, as $D/D_0 = \sqrt{H/H_0}$. With further compression, the relation displays as a linear relationship. For the same kind of gel, higher forces are needed for less swollen gels to reach the same deformation compared with gels with higher swelling ratios. This is because that the lower gel is swollen, the higher is its elastic modulus.

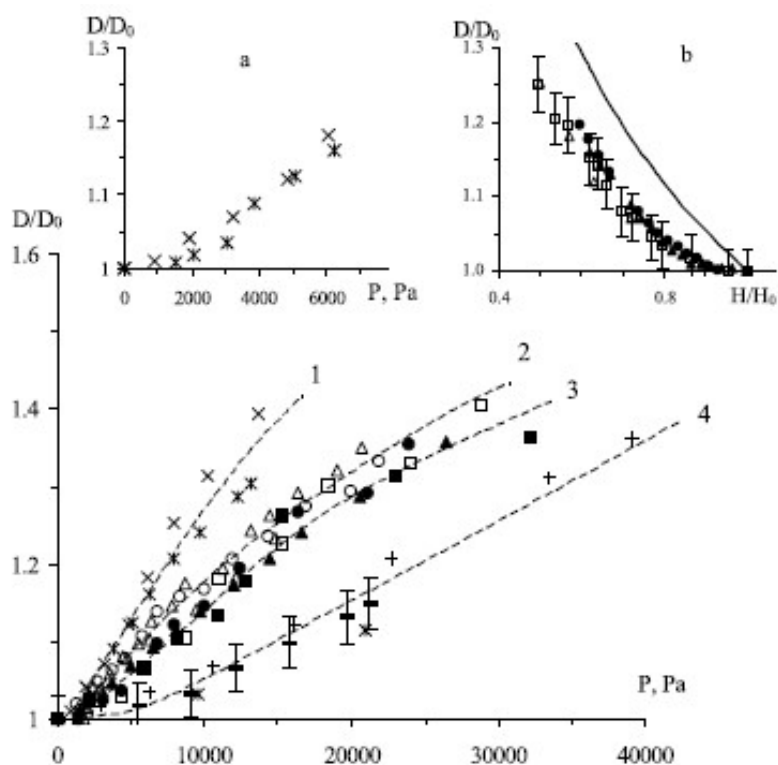


Figure 2.3 Gel deformation as a function of pressure for gels with a swelling ratio of 140 g/g (1), 100 g/g (2), 60 g/g (3), and 20 g/g (4). (a): Beginning of deformation for two potassium gel disks swollen at equilibrium (140 g/g) (b): Beginning of deformation as a function of the gap size

The authors also study the volume change as a function of applied pressure. As shown in Figure 2.4, both types of gels swollen at 140 g/g and 60 g/g lose solvent due to compression. The solvent loss can be distinguished into two stages. The first stage occurs at the beginning of the compression, in which the pressure is relatively low and a large portion of the solvent is expelled from the gel disk. Here, the authors present a terminology called “rate of release”, which represents the amount of solvent released per pressure unit. In the second stage, even the pressure is higher, less amount of water has been released compared with the first stage, and the rate of release sharply reduces as the pressure gradually increases. Thus a correlation is made: farther the hydrogel is from its initial state corresponding to $P=0$, more difficult it is to extract the solvent from it.

In the next section, the authors propose a theoretical analysis to predict the volume change of polyelectrolyte hydrogels under compression. This model is based on the Van der Waals interactions between the uncharged monomers, so it qualitatively shows that expulsion of water is more pronounced for polyelectrolyte hydrogels. For the neutral gels, the repulsion between monomers caused by the Van der Waals interactions is the main factor contributes to the gel shape and volume. When under compression, the applied uniaxial stresses restrict the repulsion, resulting in a decrease in gel volume. In the case of the polyelectrolyte hydrogels, the osmotic pressure of counterions affects the swelling ability of the hydrogels more significantly. Both the Van der Waals repulsion of the monomers and the osmotic pressure of the monomers would be diminished in this case leading to a larger amount of solvent expulsion.

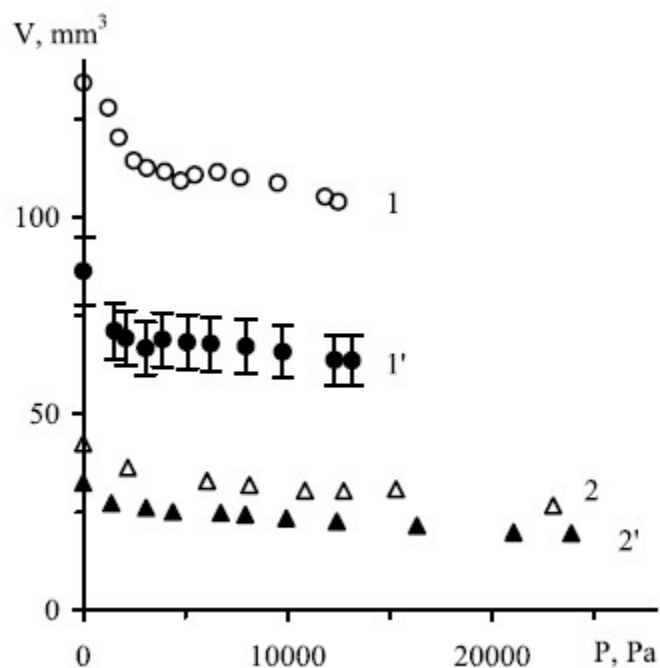


Figure 2.4 Change in the volume of the gel as a function of the pressure of potassium gels of different initial volumes. 140 g/g (1 and 1') and 60 g/g (2 and 2'). (Vervoot et al., 2005)

2.6 COMPRESSIBLE BEHAVIORS OF GELLAN HYDROGELS IN A CONSTRAINED GEOMETRY AT ULTRASLOW STRAIN RATES

Urayama, Taoka et al. (2008) study the compressible behaviors of gellan hydrogels in a constrained geometry at ultraslow strain rates. At high or moderate compression rate, the gels exhibit brittle fracture at small strains of less than 30%. At ultraslow compression rate of less than $5\mu\text{m}/\text{min}$, the gel can be compressed to 10% of its initial volume without any macroscopic fractures and they are also accompanied by a large amount of water release.

The powdered gellan is purchased from Wako Pure Chemical Ind., Japan. Resultant cylindrical gels with a diameter of 26 mm and a height of 9 mm are employed for the

measurements. The slow compression measurements are performed with a UTM-4-100 (Toyo Baldwin) which enables an ultralow crosshead speed of 0.005 mm/min. The fast compression measurements with a compression rate of more than 1 mm/min are conducted using RTM-250 (Orientec). By employing these two testers, the crosshead speed is widely varied from 0.005 to 100 mm/min. The compression tests are performed under the two boundary conditions shown as C1 and C2 in Figure 2.5. The geometry C1 employs highly viscous silicone oil attached on the lower and upper plates as lubricants, which corresponds to the conventional uniaxial compression with no restriction for radial expansion. The geometry C2 prohibits the lateral expansion by placing sandpapers between the gels surfaces and the plates. In all experiments, the gel samples are surrounded by liquid paraffin to minimize the water vaporization from the hydrogel during compression.

In this paper the stress-strain relation of the compressed gel under these two boundary conditions is discussed. The authors first study the stress-strain relation of the compressed gel under these two boundary conditions. Figure 2.6(a) shows the stress-strain curve in geometry C1 at various compression speeds (v). The gels display macroscopic fractures under small strains (ϵ_{II}) at all compression speed. The stress-strain relations are almost independent of v . Figure 2.6(b) is the stress-strain curves in the geometry C2 at various compression speed. For $v > 0.1$ mm/min, gels exhibit fractures under small strains ($\epsilon_{II} < 0.5$), which show the same manner as the gels in geometry C1. At ultralow compression speed ($v < 0.05$ mm/min), the gels are compressed to less than 10% of its initial height without any macroscopic fractures. Especially for the case that $v = 0.005$ mm/min, the gel is compressed to 2% of its initial height. (Figure 2.7a)

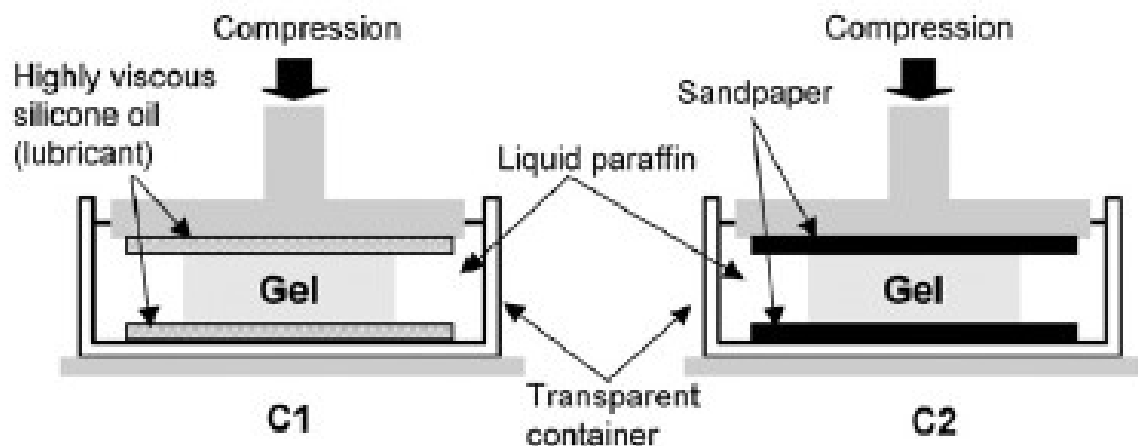


Figure 2.5 Two geometries C1 and C2 with different boundary conditions employed in compression measurements. (Urayama et al., 2008)

In this paper the stress-strain relation of the compressed gel under these two boundary conditions is discussed. The authors first study the stress-strain relation of the compressed gel under these two boundary conditions. Figure 2.6(a) shows the stress-strain curve in geometry C1 at various compression speeds (v). The gels display macroscopic fractures under small strains (ϵ_{II}) at all compression speed. The stress-strain relations are almost independent of v . Figure 2.6(b) is the stress-strain curves in the geometry C2 at various compression speed. For $v > 0.1$ mm/min, gels exhibit fractures under small strains ($\epsilon_{II} < 0.5$), which show the same manner as the gels in geometry C1. At ultralow compression speed ($v < 0.05$ mm/min), the gels are compressed to less than 10% of its initial height without any macroscopic fractures. Especially for the case that $v = 0.005$ mm/min, the gel is compressed to 2% of its initial height. (Figure 2.7a)

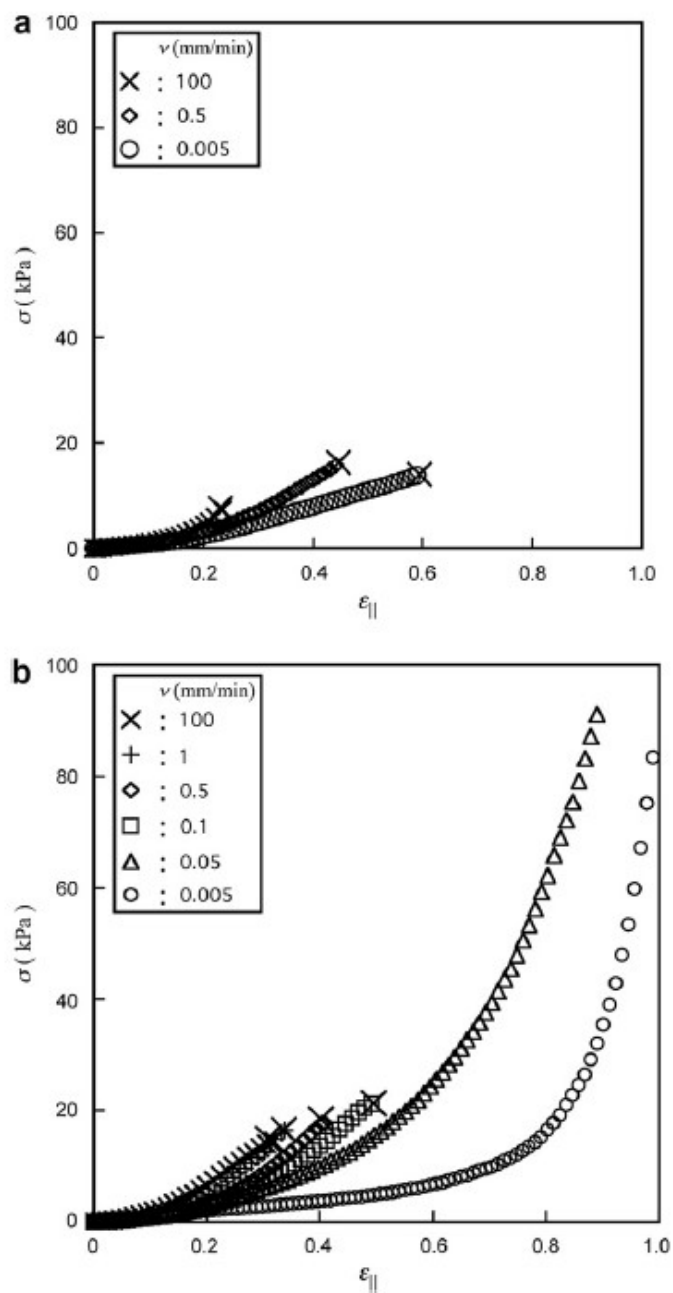


Figure 2.6 Stress-strain curves of the gellan gels compressed at various crosshead speeds under C1 and C2 conditions. The cross indicates the strain value in which the macroscopic fractures occur. (Urayama et al., 2008)

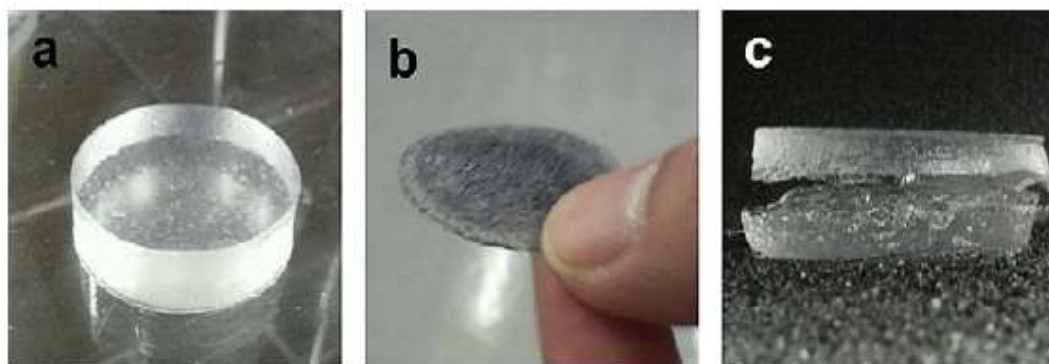


Figure 2.7 Presentation of (a) the gel sample before the compression, (b) the highly compressed gel sample without macrofractures in C2 under ultraslow compression ($v = 0.005$ mm/min), and (c) the gels reswollen by water after high compression under C2.

The remarkable deformations accompany with a large amount of expelled water from the gel under compression. Figure 2.8 shows changes in the diameter and volume of the gels as a function of ϵ_{II} in geometry C1 and C2. V_0 is the initial gel volume, and V is the gel volume under compression. A volume fraction (V/V_0) is used to interpret the volume change during compression. A gel samples underwent water expulsion regardless of the geometry. Gels under high compression speed exhibit no significant change in volume due to the early occurrence of the fracture. While the gels under low compression speed show an extremely big change in volume up to 85% before and after the compression. Gels in C2 loose more water compared with those in C1, which elucidates that the boundary conditions also have a notable influence on the volume loss. C1 leads to uniform uniaxial compression, C2 results in nonuniform compression that can be directly recognized from the convex outlines of the gel.

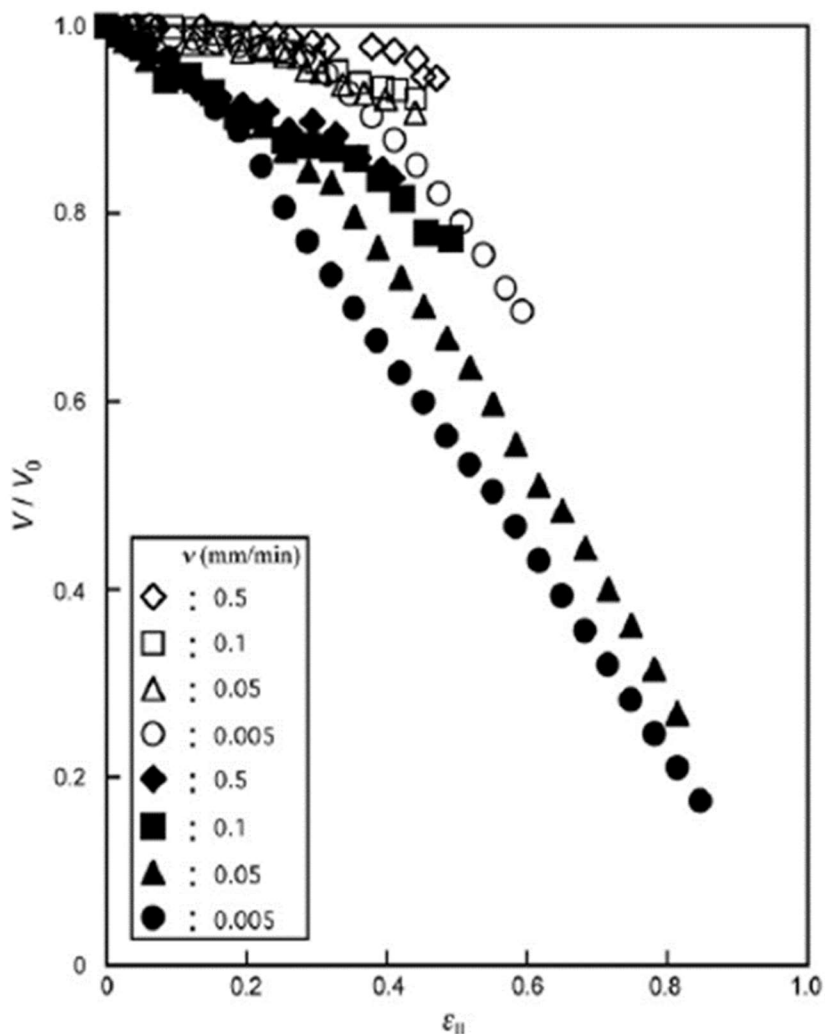


Figure 2.8 Volume variation of gellan gels during compression at various crosshead speeds under C1 and C2 conditions. (Urayama et al., 2008)

At different compression speeds and boundary conditions, gel displays distinguishable crack pattern. As seen from Figure 2.7, gels in C1 under compressions exhibit macroscopic fractures, while no perceivable fractures can be seen on gels in C2 under ultraslow compressions. However, some macroscopical fractures are found on some highly compressed gels under ultraslow compressions after being reswollen in water. This

phenomenon can be explained by the microscopic fractures formed around the central layer of the gel samples during the compressions (Figure 2.9). When the compression speed is sufficiently low, such strain concentration under C2 causes noticeable localization of the microscopic fractures around the central layer. In the reswelling process, these microscopic cracks could transform into macroscopic ones as a result of the swelling pressure. The existence of the microscopic fractures contributes to the highly compressible behavior of the gellan gels by acting as the paths for the outflow of the water.

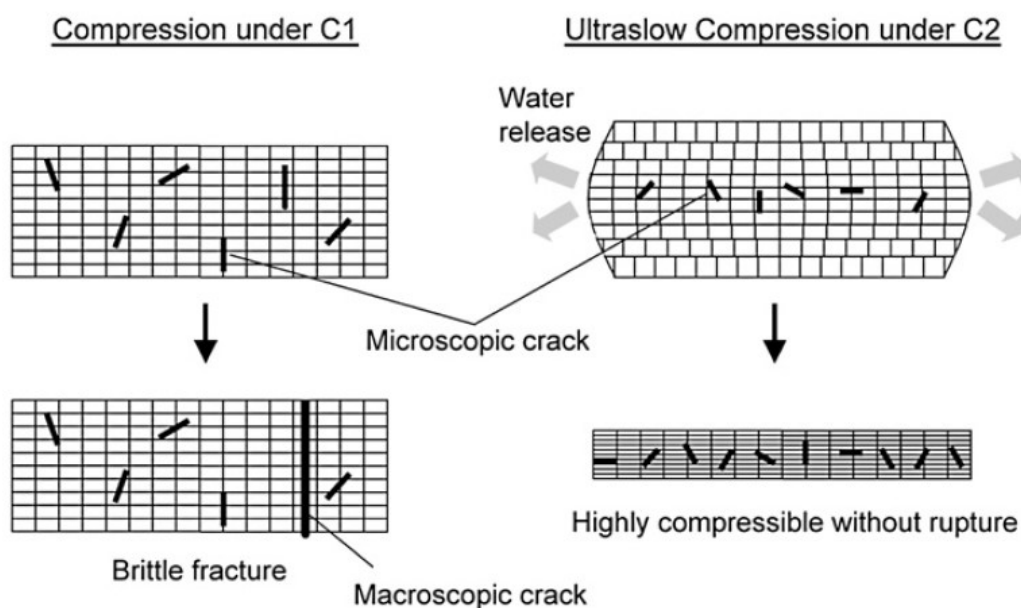


Figure 2.9 The crack pattern of gels in C1 condition under compressions (left) and that of the gels in C2 condition under ultraslow compressions (right). (Urayama et al., 2008)

2.7 VARIABLE MESO-MODEL FOR MECHANICAL AND WATER EXPELLED BEHAVIORS OF PVA HYDROGELS UNDER COMPRESSION

Zhang, Tang et al. (2017) develop a variable mass meso-model for the mechanical and water-expelled behaviors of polyvinyl alcohol (PVA) hydrogels under compression.

This model can estimate the volume loss and the stress-strain relations of hydrogels with different water contents and. Before the development of this model, the static uniaxial compression experiments are conducted to study the behaviors of PVA hydrogels in ambient conditions. During the experiments, a comparable amount of water is expelled from the gels samples that have large water content.

The PVA hydrogel used for the experiments is produced with a physical cross-linking method. The molecular weight of the PVA hydrogel varies from 89000 to 98000, and the degree of the hydrolysis is more than 99%. The diameter of the cylindrical gel samples shown in Figure 2.10 is about 33 mm and the height is 12-14 mm. These samples are cut using a freezing microtome, to make the surface even and smooth. Then, they are heated to 5 °C at a rate of 0.4 °C/min. The experiments can be separated into three subdivisions with regard to the water content (90%, 85%, and 80%, respectively).

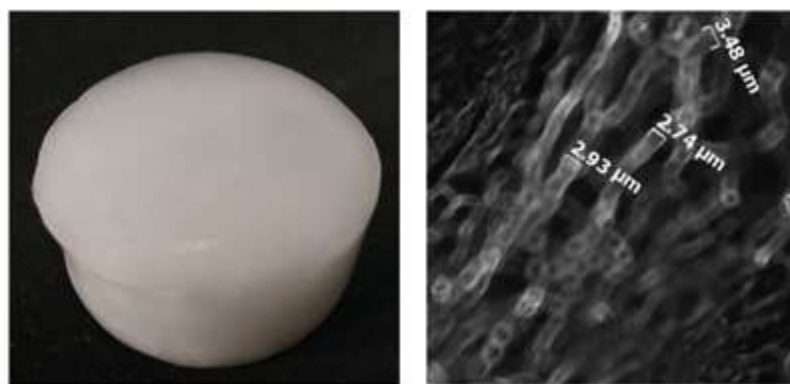


Figure 2.10 (a) A PVA gel sample; (b) A micro view of a sample with confocal laser scanning microscopy. (Zhang et al., 2017)

Uniaxial static compression tests are performed on the electromagnetic dynamic mechanical test system manufactured by CARE (China, model N-100 and the load cell is made by FUTEK, Model #: MBA500, Nonlinearity: $\pm 0.25\%$) as shown in the Figure. The maximum operating load of the load cell is 100 N. The compression applied to the gel samples is generated using a constant strain rate of 0.1%/s. A preload of 0.1 mm is applied to ensure that the plate is contacted with the gel upper surface. Because even the gel samples are cut with a freezing microtome, it is still hard to get fully flattened upper and lower gel surfaces.

Water evaporation during the compression test can be a primary factor that contaminates the accuracy of the results. Thus, each experiment is completed in no more than 10 min. Additionally, three plastic bottles are used to reduce the air flow, as shown in Figure 2.11.



Figure 2.11 The uniaxial static compression test with the electromagnetic dynamic mechanical test system. (Zhang et al., 2017)

In the next section, a model mimicking the polymer fiber frame is developed as shown in Figure 2.12. In this model, these fibers are simplified to distribute uniformly in three mutually perpendicular directions. Such a simplification avoids the difficulties of simulation caused by the randomness. These fibers construct a frame which can be viewed as composed of multiple small cubes. This model has the advantage because (1) the side surfaces consist of rectangles of the same shape only, which will bring calculative simplify; (2) the upper the lower surfaces are flat, which are needed for the compression.

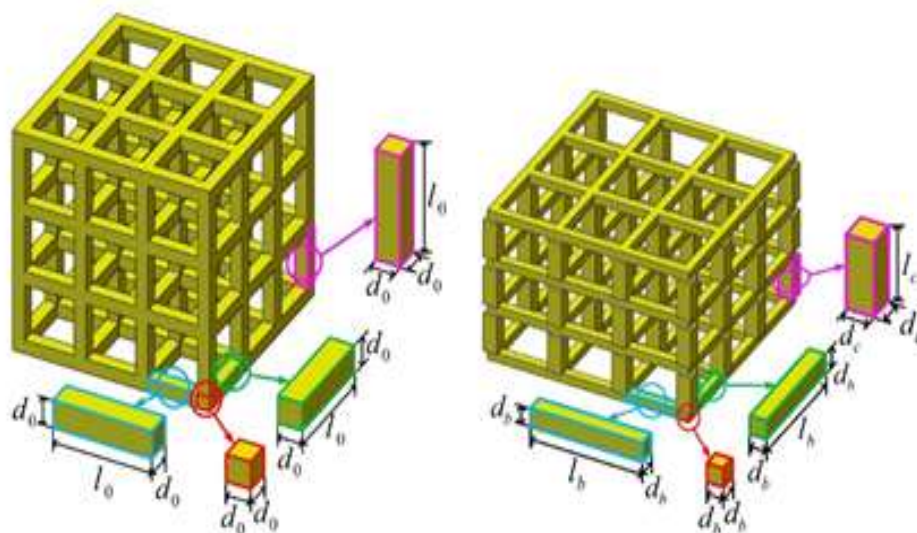


Figure 2.12 The schematic diagram of a fiber frame. (Zhang et al., 2017)

When the model is under uniaxial compression, the vertical polymer fibers are compressed and the horizontal ones are stretched. The cross-links are in triaxial stress state essentially, which causes complex deformation, and also the water expulsion. The water exists in the hydrogel can be divided into three categories: non-freezable bound water, freezable bound water, and free water. Non-freezable bound water is the water close to the polymer chains are in the same way “bound” to the polymer, thus its flowing ability is

greatly restricted. The flowing ability of the freezable bound water is also restrained by the weak hydrogel bond with fibers. These two types of water can be classified into the bound water, the free water is flowable and diffused in all pore spaces between fiber networks under the effect of osmotic pressure. Thus, the free water can be released from the hydrogel under compression and contributes to the hydrogel volume loss. Besides, a small amount of the freezable bound which changes to free water under the effect of the compression can also be expelled from the hydrogel.

In the normal state, the free water would not be expelled from the model as a result of the surface tension of water on the side surface. In this model, this surface tension functioning as a virtual membrane obstructs the outflow of the water. However, the surface tension of water is limited, thus when the model is under uniaxial static compression, the free water tends to be expelled from the hydrogel. The virtual membranes produce some bubbles on the model surface as shown in Figure 2.13 (shown as purple parts). With the increase of the load, part of the free water will break through the virtual membranes and be expelled from the model. However, the free water is not always able to be expelled from the model. At a certain strain value, the bound water around adjacent horizontal fibers on the side surface will touch with each other and therefore close the flow path of the water. In the real case, at high strain value, the gel samples are highly likely to be fractured or cracked into smaller gel particles during compression and the water would be released from the damaged gels. This model does not consider the situation of structural damage. In addition, this model neglects the volume change caused by the change in the bulk modulus of the water.

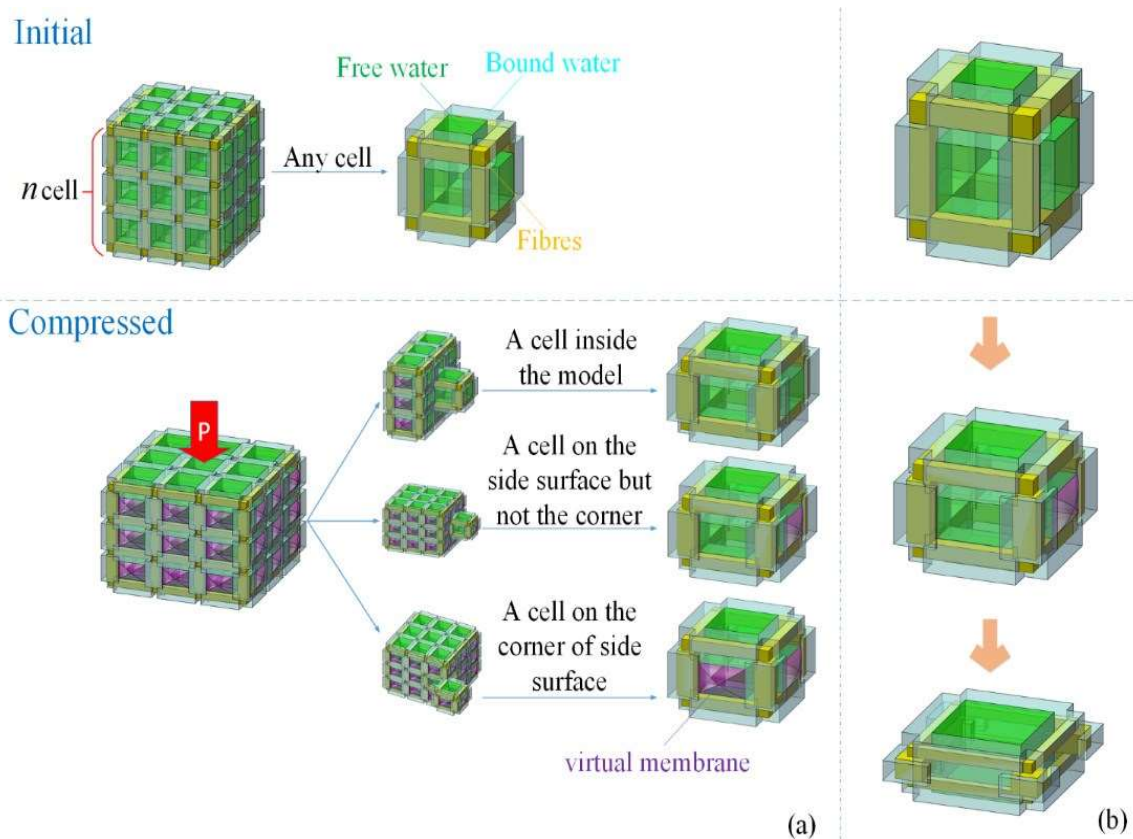


Figure 2.13 Model is constructed by three parts: free water (green), bound water (blue) and fiber (yellow). (a) When the model is compressed, cells on the side surfaces of the model produce bubbles, and there are virtual membranes (purple) that prevent the free water from flowing out freely, but a certain amount of free water is still expelled when the hydrostatic pressure reaches the surface tension of water. (b) However, if the strain reaches a certain value, the fiber with bound water will close, and the free water will no longer be expelled. (Zhang et al., 2017)

3. EXPERIMENTAL STUDIES

3.1. MATERIALS & SYNTHESIS

3.1.1. Chemicals. The hydrogels used in this study were synthesized in our laboratory. They are sodium acrylate-co-acrylamide based gels chemically cross-linked by N, N'-Methylenebisacrylamide (MBAA). Ammonium persulfate (APS) was used as the initiator for polymerization. All these chemicals mentioned above were purchased from Fisher scientific co. Sodium chloride was also purchased from Fisher Chemical co. Nitrogen gas and deionized (DI) water were provided by Missouri University of Science and Technology.

3.1.2. Gel Disk Preparation. An aqueous solution containing the monomer, crosslinker, and initiator was poured into a cylindrical test tube with an inner diameter of 12 mm as shown in Figure 3.1. Nitrogen gas was purged into the aqueous mixture to eliminate dissolved oxygen. The test tube was then placed in an oven with a temperature of 60°C to enable the solution crosslink to form the hydrogel. After 6 hours, the gelation was accomplished and the test tube was taken out from the oven. Gel disks with heights of around 2 mm were cut from the bulk gel and then immersed in the brine until reaching fully swollen states. The brine was refreshed every day to washout the unreacted chemicals. For each factor attributes to the change in the gel composition, 5 samples were prepared as shown in Table 3.1.

Table 3.1 Gel samples with different gel formulation.

Sample number	Brine type (wt %)	Crosslinker concentration (wt %)	Monomer concentration (wt %)
1	DI water	0.03	20
2	0.1	0.06	30
3	0.25	0.12	40
4	1	0.18	50
5	10	0.24	60

The detailed preparation processes are as follows:

1. Prepare an aqueous solution containing the chemicals mentioned above in a test tube with an inner diameter of 12 mm as shown in Figure 3.1.
2. Place the test tube in an oven with a temperature of 60°C and let the solution crosslink to form the hydrogel.
3. Cut the bulk gel into small gel disks with heights of around 2 mm.
4. Immerse the gel disks in the brine, and refresh the brine once a day. This process aims to remove any soluble impurities and let the gel disk adsorb water.
5. The fully swollen state of the gel is determined by measuring the weight of the gel disk each day.

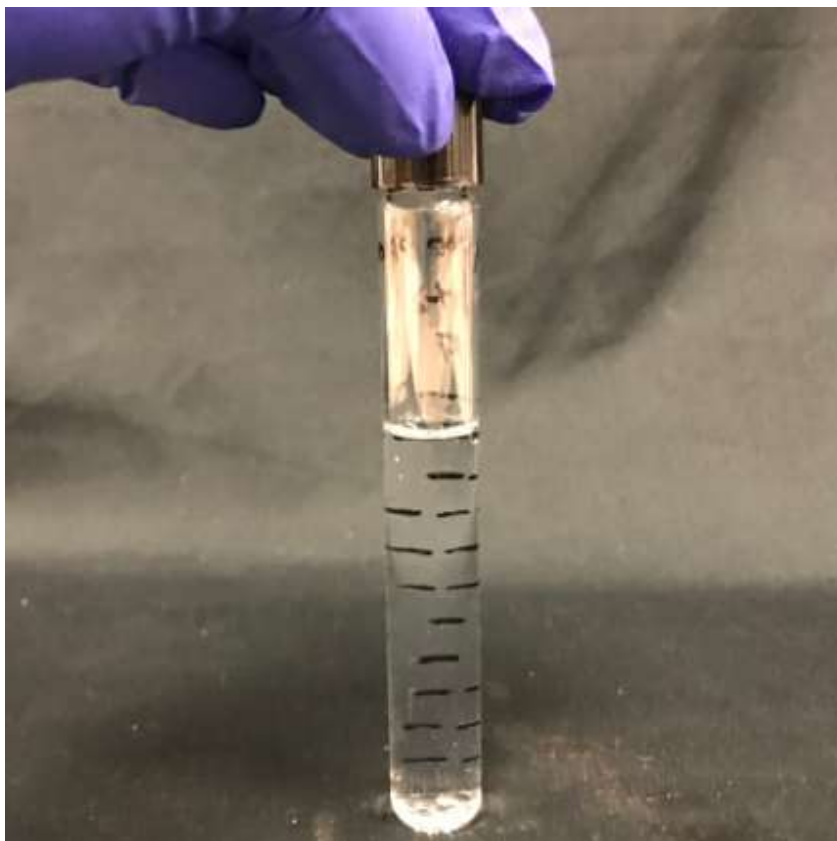


Figure 3.1 Gelation in the test tube

3.2. METHOD

3.2.1. Swelling Degree Measurement. The swelling degree of the gel here was defined as the ratio of the weight of the gel in the fully swollen state to that of the gel in the dry state. After reaching the fully swollen state (Figure 3.2 a), the gel was taken out to measure the weight. Then it was placed in a hood under room temperature to dry until all the water in the gel was expelled and the weight of the gel in the dry state can be thus measured (Figure 3.2 b).



Figure 3.2 Presentation of (a) the gel disk in a fully swollen state and (b) gel in the dry state

3.2.2 Compression Test. The compression experiments were conducted with a HAAKE™ MARST™ 40 and 60 rheometer, manufactured by Thermo Scientific™ at a temperature of 25°C. As shown in Figure 3.3, the gel was put on the lower plate. The upper plate moved vertically at a constant speed to generate the uni-axial compression. Conventional wisdom suggests using sandpapers coated on the plates to help fix the gel. However, this operation has the risk of bringing serious damage to the gel surface, and thus results in an early breakage of the gel disk. Therefore, a pre-test was conducted to evaluate the gel slippage under the plate-plate movement. No slippage was observed during the pre-tests. That is to say, the gel disk can be fixed between the upper and lower plate without the help of the sandpaper. Therefore, all of our experiments were conducted without coating sandpaper onto the plates.

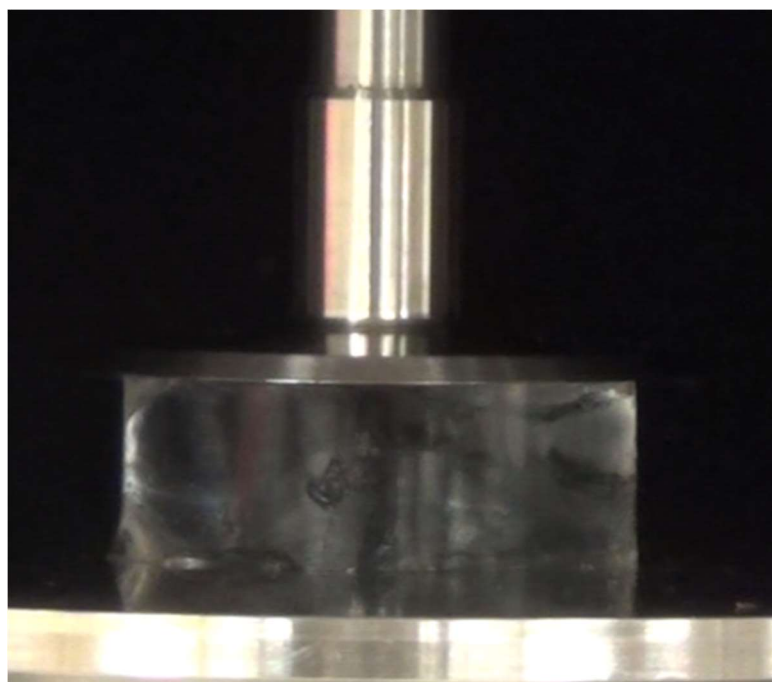


Figure 3.3 The gel disk placed between the upper and lower plates.

During the experiments, the gradually increased force to cause the deformation was measured by the rheometer. A camera was used to monitor the change in the lateral dimension of the gel disk. Vervoort, Patlazhan et al. (2005) measured the diameter of the gel disk at sample half-height during the experiment and the volume of the gel disk was calculated by applying the formula for the volume of a cylinder. All data discussed here corresponds to the gel samples before any breakage. In our study, the gel disk under compression was also roughly considered as a cylinder, however, a different way to measure the diameter was applied. As being compressed, gel deforms and expands laterally showing a concave shape (see Figure 3.4) due to the friction between the plates and gel surfaces. Using the disk diameter at the middle-height may cause a serious measurement error. Moreover, a gel under compression typically reduces less than 10% of its initial volume as a result of the water expulsion. Even a small measurement error will dramatically compromise the accuracy of the results. Therefore, an average diameter was applied to improve the accuracy of the results in our experiments, which is the average of the diameter measured at half-height and full-height.

The speed of the upper plate mainly depends on water evaporation and fracture behavior of the gel disk at different strain rate. As the objective of this study is to investigate the water expulsion from hydrogel under compression, the water evaporation should be avoided during the experiments. In some publications, the gel was placed in a bath of solvent to prevent water from escaping from the gel due to the evaporation. However, it brings the difficulty in measuring the change in gel volume and there is no way to see the water released from the gel. Thereby, our experiments have to be conducted in the air. To minimize water evaporation, the experiment should be completed in a short time. Knowing

that high strain rate could lead to the early breakage of the gel disk, a moderate or low compression speed is preferred. Taking these two factors into account, experiments were conducted in a duration of 10 mins.

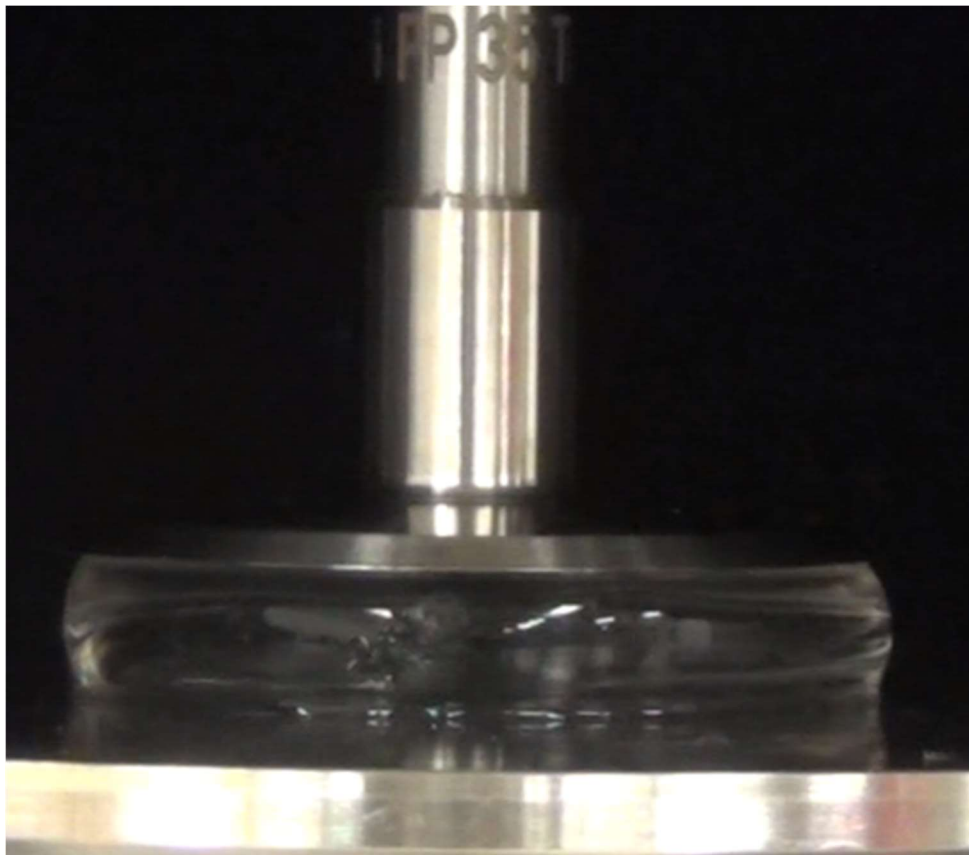


Figure 3.4 The concave shape of the compressed gel disk

The gel disks we used were initially cut in a uniform size, with a diameter of 12 mm and a height of 2 mm. However, because of gel formulations or solvent types, gel disks after swelling were of uneven sizes. Thus we were not suggested to simply set up a constant plate speed for all sets of experiments. To achieve equalized strain rates, a duration for the upper plate getting attached with the lower plate was used, which is 10 mins as mentioned

above. Moreover, once the gel expands and moves out of the cover of the upper plate, a shear force is generated between the edge of the upper plate and the gel. In order to avoid this, a glass chip was attached below the upper plate for some experiments in which the gels have larger diameters. As seen from Figure 3.5, the glass chip has a larger diameter compared with the upper plate, which allows more expansion of the gel disk.



Figure 3.5 Glass chip with a larger diameter used during the compression test

3.2.3 Measurement of Storage Modulus and Loss Modulus. Test samples with a diameter of 10 mm and a height of 1.5 mm were cut from the gel disk before and after the compression, respectively. Once the gel is damaged, it cannot be used for the compression test. Thus, the test sample of the gel disk before the compression was taken from another gel disk. The storage modulus and the loss modulus of the gel was measured with a HAAKE™ MARST™ 40 and 60 rheometer, manufactured by Thermo Scientific™. The objective of this step is to characterize the mechanical property of the gel disk before and after the compression test.

4. EXPERIMENTAL STUDIES

4.1. EFFECT OF BRINE CONCENTRATION

As shown in Table 4.1, Brines including DI water and sodium chloride solutions with different concentrations are used for swelling of the gel disks. The gel immersed in the DI water shows great absorption capacity. The swelling degree decreases when the NaCl concentration increases, indicating that the screening effect of the ions on double layer repulsions between polymer chains. Since the gel contains hydrophilic polymers, some water is inevitably trapped in the gel. These water adsorbed to the polymer backbones cannot be completely expelled from the gel as the preswollen gel dries, thus complicating the measurement of the degree of swelling. However, only a small amount of water can be trapped, so it was ignored in our study. The swelling degree decreases steeply in the range 0.1%-1%, while only a subtle change in swelling degree was observed when the concentration of NaCl increases from 1% to 10%. Thus we can infer that the minimum critical concentration, in which the electrostatic interactions is completely screened off, is in the range 1% to 10%. Figure 4.1 shows the gel volume loss as a function of pressure. Volume loss is a term that represents the amount of water released from the gel disk in percentage, which can be defined as: $(V_i - V)/V_i \times 100\%$. Where V_i is the initial volume of the gel disk and V is that of the gel disk under compression. The pressure is calculated with the normal force generated by the rheometer and the cross-section area of the gel disk. The normal force is automatically given by the rheometer, and the cross-section area can be calculated from the average diameter of the gel disk.

Table 4.1 The swelling ratio of gels swollen in different brines

brine type	Swelling ratio
DI	149.648
0.1%Nacl	49.195
0.25%Nacl	33.465
1%Nacl	17.415
10%Nacl	16.8718

As seen in Figure 4.1, the gel disk swollen in DI water loses water immediately after the normal force is generated. The volume loss increases at elevated pressures during the compression. This water release process ends up a volume loss of about 6% when the pressure reaches up to 14000 pa. The gel disk is then broken with a fracture at this pressure and thus the experiment is stopped. This experiment ends earlier compared with the others. As the gel adsorbs a noticeable amount of water when being immersed in DI water, the polymer chains have been stretched, resulting in low gel strength.

As the NaCl concentration increases, the degree of gel swelling decreases, and thus the gel tensile strength increases. That explains that more data points exhibit for gel swollen in highly concentrated NaCl solutions. For gel swollen in 10% NaCl solution, the experiment stops at a pressure of about 56,000 pa. This is not caused by the gel breakage but the limited normal force that the rheometer can provide, which means the gel is able to withstand higher pressure. The water is released rapidly at the beginning and this stage is so-called 'quick release stage'. After the quick release stage, the rate of release (volume

loss per pressure unit) reduces gradually as the pressure increases. Curves do not pass through the zero point, due to the measurement errors. In fact, it is difficult to start recording at the point that the upper plate touches the surface of the gel disk. Thus some data point at the beginning could be missed, leading to the deviation.

Zhang, Tang et al. (2017) developed a model that considers the hydrogel is composited by finite cells constructed by fibers, bound water, and free water. Researchers believed that only the free water confined in the cells can be expelled and the bound water will keep surrounding the fibers even being deformed. During the compression, the flow path for releasing free water is diminished in a complex way. That explains the decreasing rate of release aforementioned. If the gel is highly deformed, the bound water has a chance to attach to each other, and thus the flow path is fully closed. However, gels are essentially broken or fractured before reaching such a great deformation.

Realistically, the hydrogel forms with network defects, leading to the gel inhomogeneity. The scattering intensity from the polymer solution is always larger than that from the gels, manifesting the gel inhomogeneity (Kizilay and Okay 2003). Thus, the fibers distribute nonuniformly in the gel due to the gel inhomogeneity, and this model should be carefully used according to the inhomogeneity of the gel. This decreased release rate is also caused by the elastic properties of the gel. When the hydrogel is subjected to compression or tension, the strain increases with the increased stress in a polynomial fashion (Okay and Durmaz 2002). In another word, the stress must be increased at a high rate with respect to the strain. Hence, the gel disk is less readily to be further compressed to release the water.

During the experiments, no threshold pressure for water release was observed. Theoretically, the compression leads to a gel deformation, causing a significant change in minimum Gibbs free energy. An entropy force, therefore, exists to resist the deformation leading to a threshold pressure for water to release. However, in our experiments, the force acting upon the gel disk almost decreases at the same time as it is generated due to the water release, which indicates there is no threshold for water to release. That may be because the entropy force is too small to be detected by the rheometer. It is found that the gel disk swollen in higher concentration NaCl solutions releases less water. This is reasonable because as the concentration increases, the resistance of the gel to the uni-axial compression increases.

The compression experiments are dynamic processes, directly comparing volume losses at certain pressures is an improper way to evaluate the gel behavior under compression. However, it is obvious that the higher the NaCl concentration, the less the volume loss is. One explanation is that the gel has a smaller pore size when the concentration of the NaCl solution increases. The porous structure can easily be affected by the affinity of the hydrogels for the aqueous environment where they are swollen (Hoare and Kohane 2008). Gels swollen in high salinity brine tend to adsorb less water and have smaller pore sizes, which restricts the gel from releasing water. Another decisive factor for gel volume loss is the gel stiffness. The gel stiffness increases with increasing concentration of NaCl. Thus, the gel with higher stiffness requires larger stress to reach the same strain, compared with others.

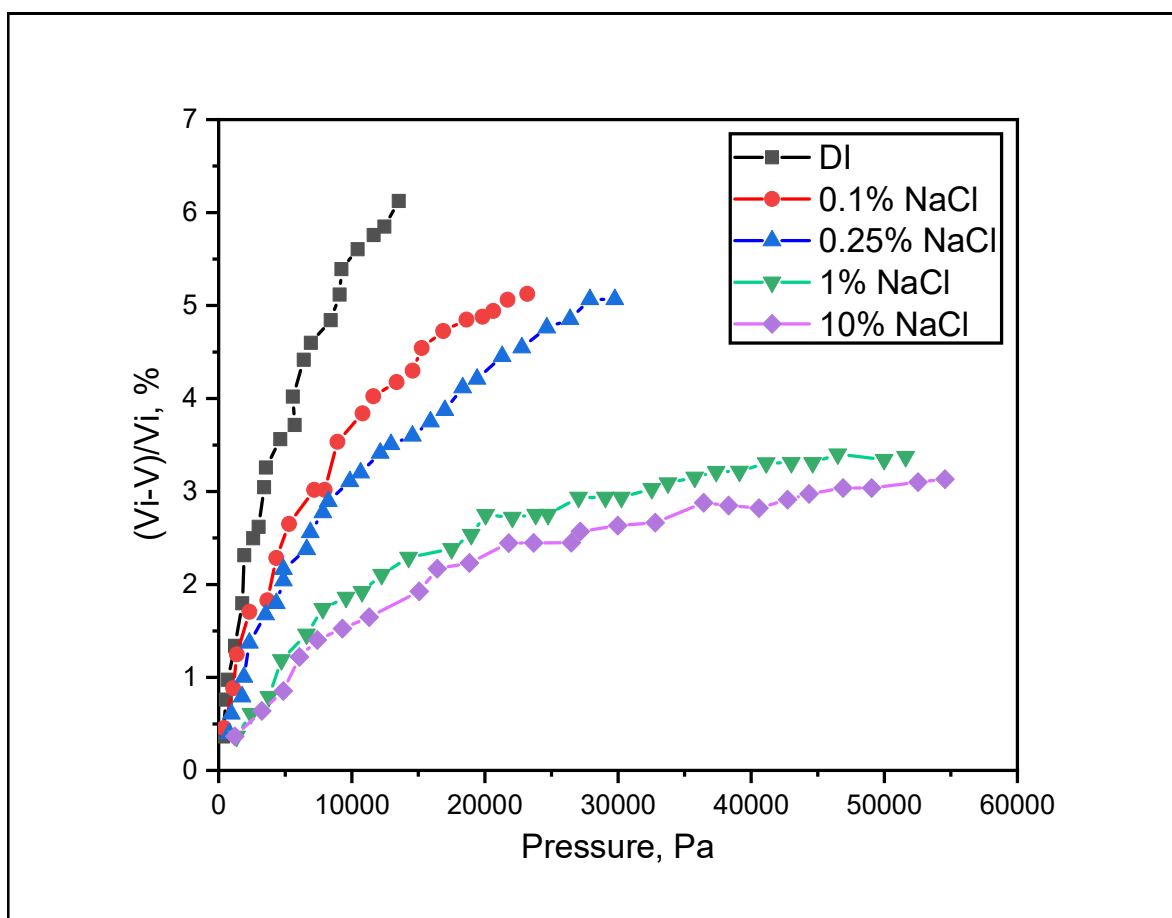


Figure 4.1 Volume loss as a function of the pressure for gels swollen in different brines

The strength of the gel can be revealed by the G' measured with the rheometer as shown in Figure 4.2 (a). After compression tests, the G' of gels swollen in different brines decrease, illustrating gels undergo strength reduction during the course of releasing water. However, in our previous studies, results show the gel that loses water due to either the chemical action or the shear stress exhibits an increase in the gel strength. Thereby, the reduction of the gel strength is not caused by the water expulsion, and there must be other factors diminishes the gel strength. In fact, during the compression, even no fracture or crack was observed on the gel disk, some microscopic cracks could be formed at the central

part of the gel disk (Urayama, Taoka et al. 2008). Thus, the loss modulus of gels before and after compression is measured to address this problem. As seen from Figure 4.2 (b), for each gel sample, an increase in G'' was observed, which means the gel is more viscous after the compression test. That indicates the gel structure is damaged during the compression, leading to the reduction of the gel strength. Therefore, there are two mechanisms impact the gel strength under compression: water loss increases the gel strength and structural damage decreases the gel strength. Here, results show that the gel strength is reduced after compression because the structural damage is the dominant factor.

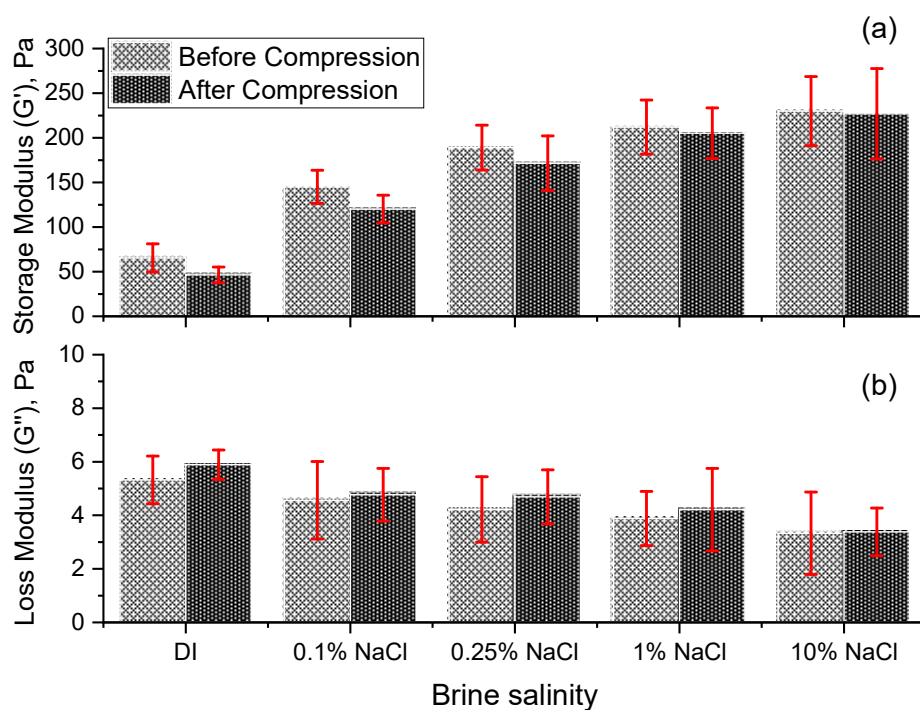


Figure 4.2 Change in (a) storage modulus (G') and (b) loss modulus (G'') for gels swollen in different brines

4.2. EFFECT OF CROSSLINKER CONCENTRATION

In this section, the gel samples synthesized for the compression experiments have the same formulation except for crosslinker concentration. As shown in Table 4.2, five crosslinker concentrations were selected for the compression test. After polymerization reactions, the gel disk was immersed in DI water until reaching a fully swollen state. The crosslinker concentration has an adverse impact on the swelling degree of the gel disk because an increase in the crosslinking density will limit the diffusion of water into the gel network. Increasing crosslinker concentration from 0.03 % (w/w) to 0.24 % leads to a dramatic reduction of the gel swelling ratio from 149 to 48.

Table 4.2 The swelling ratio of the gel with different initial crosslinker concentration

Cl concentration (%)	Swelling ratio
0.03	149.997
0.06	142.487
0.12	103.87
0.18	76.414667
0.24	48.336484

As seen from Figure 4.3, the gel disk with a crosslinker concentration of 0.03 % (w/w) shows an early breakage. When the gel disk was taken out from the DI water, some sticky transparent liquid was found on the surface of the gel disk. This is caused by the low

crosslinking density due to the low crosslinker concentration. The gel was severely soft, even can be broken if being caught improperly by tweezers. Thus, the gel only withstood up to around 9500 psi and broke into small particles during the experiment. Gels synthesized with higher crosslinker concentration are able to endure higher pressure. For gel with crosslinker concentrations of 0.18 and 0.24 % (w/w), no crack was found during the test.

The volume loss is lower when the initial crosslinker concentration used for gel synthesis increases. Except for the smaller performed pore size and higher stiffness of the gel with respect to the decreasing swelling degree, bound/free water fraction also contributes to diminishing volume loss. Katime, Quintana et al. (2006) studied the effect of crosslinking concentration on mechanical properties in acrylic acid-co-methyl methacrylate hydrogels. It was found that the crosslinker concentration has an effect on the portions of the free water volume and the bound water volume to the gel volume. At a constant temperature, a higher crosslinker concentration generally leads to a gel with lower water content, a higher percentage of bound water, and a lower percentage of the free water. When the crosslinker concentration exceeds the critical concentration, these values will tend to be stable. Based on the results in Table 4.2, the chosen crosslinker concentrations for our experiments are less than this critical concentration. Generally, only the free water tend to be released under the compression, and the bound water surrounded the fibers has an effect on the flow path of the free water. Thus, a lower percentage of free water can significantly reduce the volume loss of the gel disk during the compression. Additionally, a higher percentage of the bound water decreases the cross-sectional area of the flow path, bringing difficulties for water expulsion. However, the differences in volume losses

between gels with different crosslink concentrations are not as large as we expected. This will be systematically explained in the next section that studies the gel strength reduction after the compression.

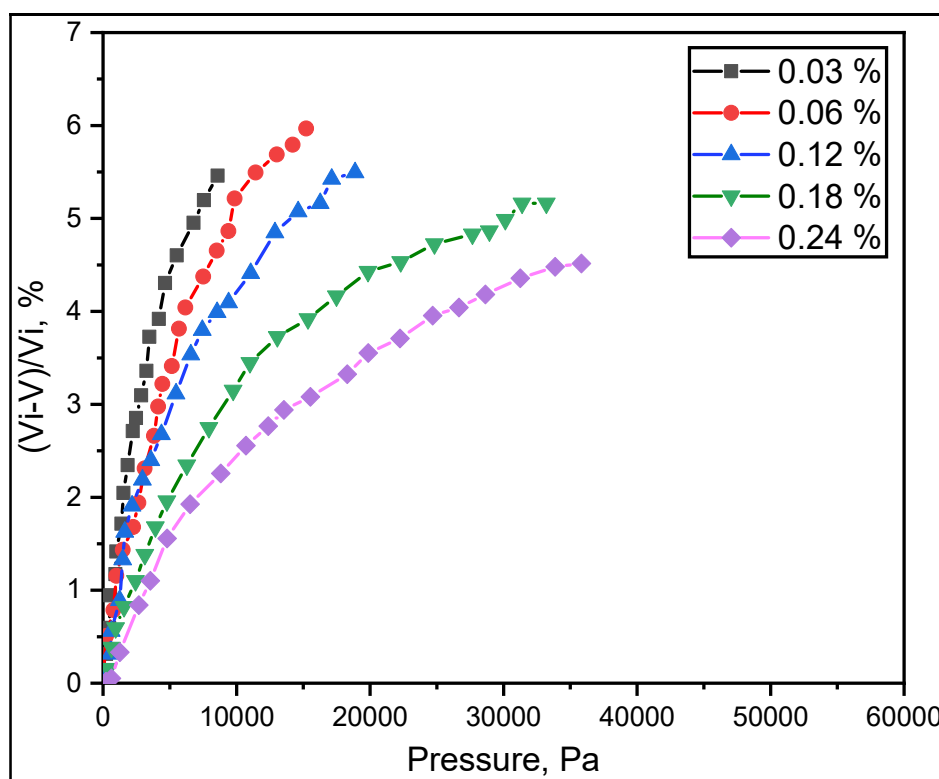


Figure 4.3 Volume loss as a function of pressure for gels with different initial crosslinker concentrations

After compression, the reduction of G' also shows for each gel with different crosslinker concentrations (see Figure 4.4 (a)). On the other hand, the G'' of each gel increases as shown in Figure 4.4 (b) Gel become less elastic and more viscous, indicating damage to the gel network. Since no visible structural damage on the gel body, some microscopic cracks may be formed. As the crosslinking density of the gel increases, the gel

becomes unstable and brittle. Thus, it increases the risk of forming microscopic cracks. The high gel strength and such a low strain rate prohibit the growth of these microscopic cracks, avoiding the genesis of the macroscopic fractures. These microscopic cracks act as the additional flow paths for releasing free water (Urayama, Taoka et al. 2008). A higher crosslinker concentration decreases the volume loss due to the less free water and the restricted natural flow paths, however, also creates extra flow paths for free water by forming more microscopic fractures. That explains why the differences in volume loss are less than we predicted in the previous section.

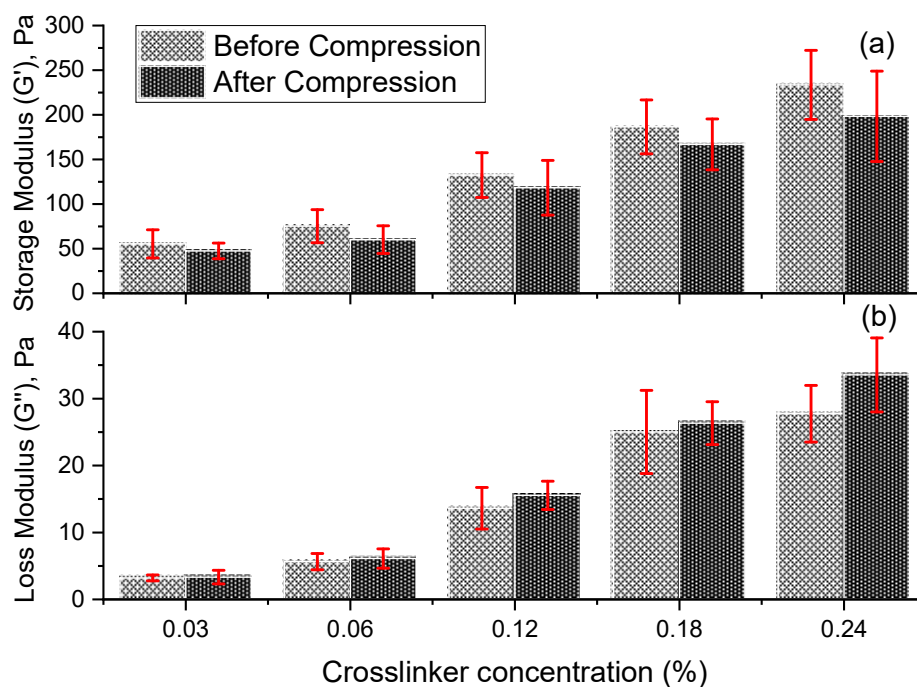


Figure 4.4 Change in (a) storage modulus (G') and (b) loss modulus (G'') for gels with different crosslinker concentrations

4.3. EFFECT OF MONOMER CONCENTRATION

In this section, the gel with different monomer concentrations was used to study the effect of the monomer concentration on the water expulsion of the gel under the compression. The concentrations of the initiator and the crosslinker concentration were held at a constant value for all syntheses. The ratio of Acrylamide to Sodium acrylate was also kept as a constant value of 9. As the monomer concentration used for the gel synthesis increases, the swelling ratio of the gel decreases, which is what we expected. The swelling ratio of the gel with the monomer concentration of 30 % is only 10 less than that of the gel with the monomer concentration of 20 %. While the swelling ratio of the gel with the monomer concentration of 40 % is 50 less than that of the gel with the monomer concentration of 50 %. That appears there is no linear relationship between the gel swelling ratio and the monomer concentration. The gel synthesized with the initial monomer concentration of 60 % showed a swelling ratio of roughly 95, which was an exception to the regulation that the swelling degree of the cationic acrylamide-based hydrogel declines with rising monomer concentrations. Thus, the gels with the initial monomer concentrations of 60 % and above were not considered for this study. Technically, we were able to synthesize the gel with the monomer concentration of less than 20 %. However, the gels were too fragile to be subjected to mechanical testing.

As seen from Figure 4.5, at the pressure of 9000 psi, the volume loss of the gel with the monomer concentration of 20 % is roughly 6 % of the initial gel volume, and the gel disk was broken at this pressure. During the synthesis, because of the low monomer concentration, the solution tends to be highly diluted. Crosslinks may be wasted in network defects such as unreacted pendant double bonds and elastically ineffective loops. The

growing chains are dilute and chains crosslink upon themselves to form loops, further wasting some crosslinks. Therefore, the crosslinking density of this gel may be less than the nominal crosslinking density (Baker, Hong et al. 1994), and the gel is thus weaker than others. The flow of water is less impeded by a loose polymer network structure.

Table 4.3 Swelling ratio of gels with different initial monomer concentration

Monomer concentration	swelling ratio
20%	153.245
30%	144.52
40%	91.54
50%	62.48

As seen from Figure 4.5, at the pressure of 9000 psi, the volume loss of the gel with the monomer concentration of 20 % is roughly 6 % of the initial gel volume, and the gel disk was broken at this pressure. During the synthesis, because of the low monomer concentration, the solution tends to be highly diluted. Crosslinks may be wasted in network defects such as unreacted pendant double bonds and elastically ineffective loops. The growing chains are dilute and chains crosslink upon themselves to form loops, further wasting some crosslinks. Therefore, the crosslinking density of this gel may be less than

the nominal crosslinking density (Baker, Hong et al. 1994), and the gel is thus weaker than others. The flow of water is less impeded by a loose polymer network structure.

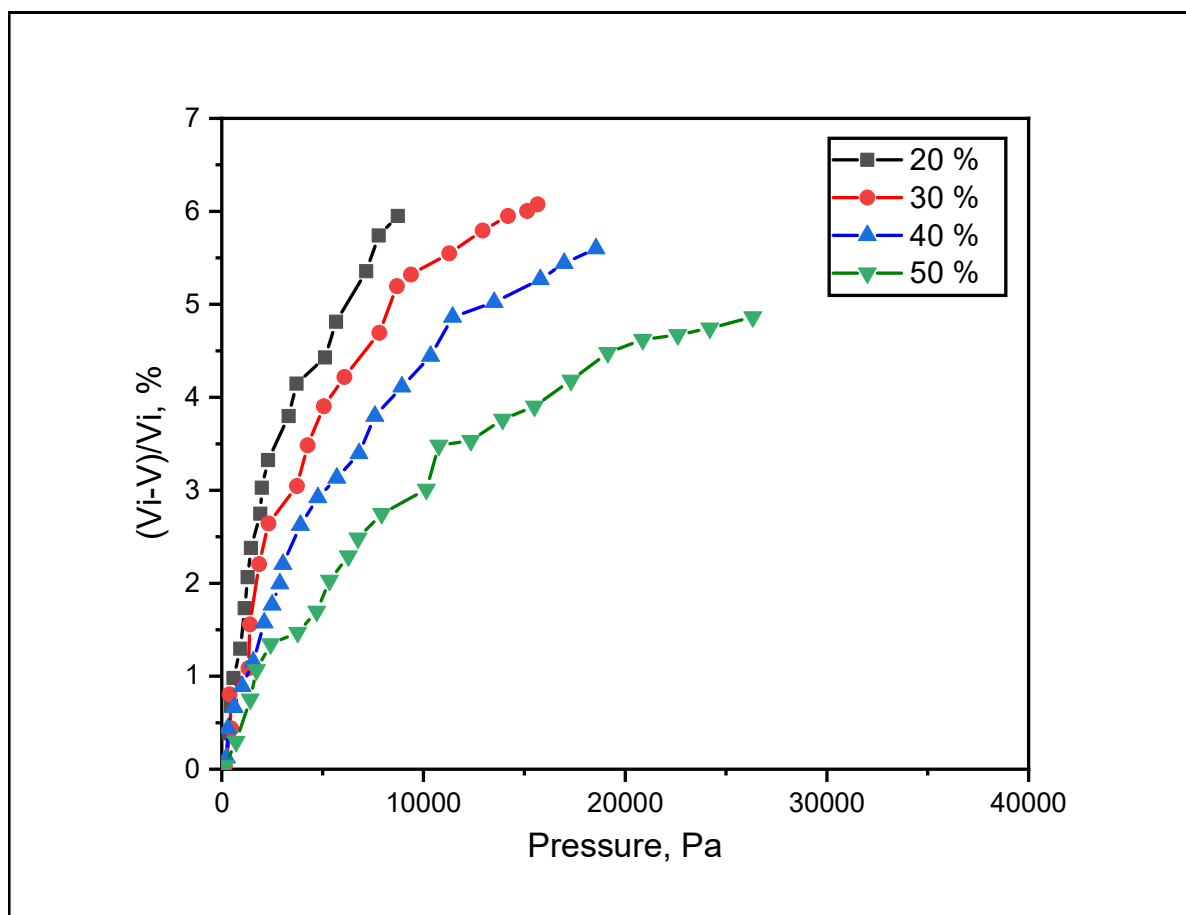


Figure 4.5 Volume loss as a function of pressure for gels with different initial monomer concentration.

The results demonstrate that the gel with a higher monomer concentration releases less water under compression. Besides the less preformed size and the higher gel stiffness, monomer concentration also influence the gel dehydration in a complex way. At a low monomer concentration, the loose polymer network structure tends to lead a greater volume loss. As the monomer concentration slightly increases, it is likely the crosslinking

efficiency improves, and the crosslink density of the gel increases (Kizilay and Okay 2003). Gel becomes stiffer and the gel structural is denser. Moreover, a higher crosslink density also leads to less free water because the amount of bound water increases with the crosslink density. As the monomer concentration keep increasing, it is likely the gel has a low crosslink density because the crosslinker concentration is constant.

As seen from Figure 4.6, a reduction in G' is observed for each gel sample after the compression experiments. As expected, G'' of gels with different monomer concentration increase, indicating the structural damage of the gel network. The existence of the microscopic fractures reduces the gel strength and creates more flow path for water to release.

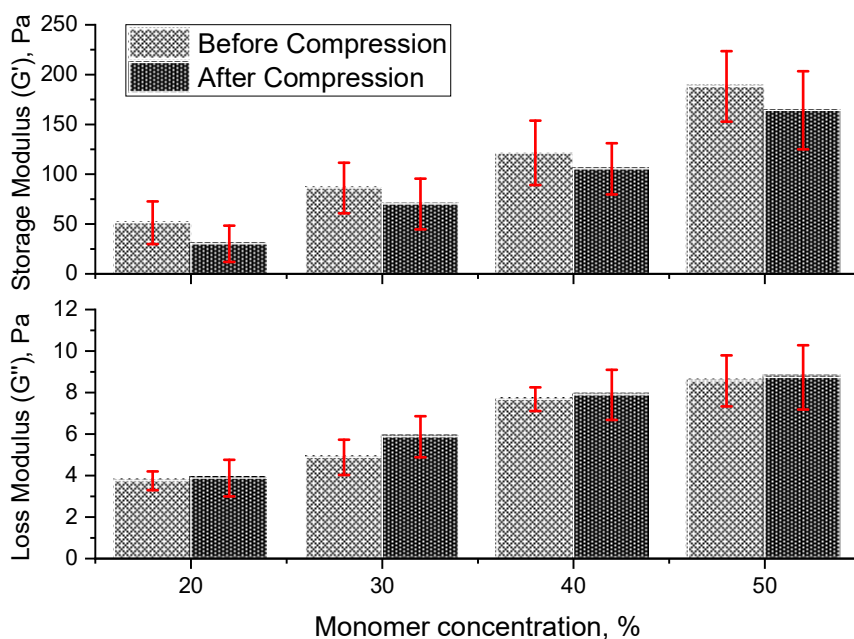


Figure 4.6 Change in (a) storage modulus (G') and (b) loss modulus (G'') for gels with different initial monomer concentration

5. CONCLUSIONS

In this study, the compression experiments were conducted to study the effect of the change in gel composition and brine concentration to gel dehydration under uni-axial compression. The G' and G'' of the gel before and after the compression were measured to evaluate the gel mechanical property. This work is of great importance for gel treatment for conformance control. By knowing the gel dehydration varies with the gel composition and brine concentration, operators are able to better manage gel treatment projects.

In a field-scale gel treatment, gels placed in the reservoir are subjected to a higher pressure and a longer compression time. The dehydration could be significant and the volume loss can be much greater than the experimental result. Works regarding gel dehydration under higher pressures and lower strain rates should be done in the future. However, this work is of great importance for gel treatment for conformance control. By knowing the gel dehydration varies with the gel composition and brine concentration, operators are able to better manage gel treatment projects.

REFERENCES

- Bai, B. and Zhang, H. (2011). "Preformed-particle-gel transport through open fractures and its effect on water flow." *SPE Journal* 16(02): 388-400.
- Baker, J. P., et al. (1994). "Effect of initial total monomer concentration on the swelling behavior of cationic acrylamide-based hydrogels." *Macromolecules* 27(6): 1446-1454.
- Brattekkås, B., et al. (2018). Solvent Leakoff During Gel Placement in Fractures: Extension to Oil-Saturated Porous Media. SPE Improved Oil Recovery Conference, Society of Petroleum Engineers.
- Chauveteau, G., et al. (2000). Controlling gelation time and microgel size for water shutoff. SPE/DOE improved oil recovery symposium, Society of Petroleum Engineers.
- Feng, Y., et al. (2003). Characteristics of microgels designed for water shutoff and profile control. International Symposium on Oilfield Chemistry, Society of Petroleum Engineers.
- Geng, J., et al. (2018). Experimental Study on Charged Nanogels for Interfacial Tension Reduction and Emulsion Stabilization at Various Salinities and Oil Types. SPE Asia Pacific Oil and Gas Conference and Exhibition, Society of Petroleum Engineers.
- Hoare, T. R. and D. S. Kohane (2008). "Hydrogels in drug delivery: Progress and challenges." *Polymer* 49(8): 1993-2007.
- Katime, I., et al. (2006). "Synthesis and Properties of pH - and Temperature - Sensitive Poly [(N - isopropylacrylamide) - co - (2 - methylenebutane - 1, 4 - dioic acid)] Hydrogels." *Macromolecular Chemistry and Physics* 207(22): 2121-2127.
- Kizilay, M. Y. and O. Okay (2003). "Effect of initial monomer concentration on spatial inhomogeneity in poly (acrylamide) gels." *Macromolecules* 36(18): 6856-6862.
- Nakamura, K., et al. (2001). "The influence of compression velocity on strength and structure for gellan gels." *Food Hydrocolloids* 15(3): 247-252.
- Nguyen, T. Q., et al. (2004). Effect of composition of a polyacrylamide-chromium (iii) acetate gel on the magnitude of gel dehydration and disproportionate permeability reduction. SPE/DOE Symposium on Improved Oil Recovery, Society of Petroleum Engineers.

- Okay, O. and S. Durmaz (2002). "Charge density dependence of elastic modulus of strong polyelectrolyte hydrogels." *Polymer* 43(4): 1215-1221.
- Reddy, R. N. and R. G. Reddy (2003). "Sol-gel MnO₂ as an electrode material for electrochemical capacitors." *Journal of Power Sources* 124(1): 330-337.
- Seright, R. (1995). "Gel placement in fractured systems." *SPE production & facilities* 10(04): 241-248.
- Seright, R. (1999). "Polymer gel dehydration during extrusion through fractures." *SPE production & facilities* 14(02): 110-116.
- Seright, R., et al. (1997). Sizing gelant treatments in hydraulically fractured production wells. *SPE Annual Technical Conference and Exhibition, Society of Petroleum Engineers.*
- Seright, R. S. (1998). Gel dehydration during extrusion through fractures. *SPE Rocky Mountain Regional/Low-Permeability Reservoirs Symposium, Society of Petroleum Engineers.*
- Seright, R. S. (2001). Gel propagation through fractures. *SPE Production & Facilities*, 16(04), 225-231.
- Seright, R. S. (2003). Conformance improvement using gels, *New Mexico Institute of Mining and Technology (US).*
- Seright, R. S. (2003). An alternative view of filter-cake formation in fractures inspired by Cr (III)-acetate-HPAM gel extrusion. *SPE production & facilities*, 18(01), 65-72.
- Urayama, K. and T. Takigawa (2012). "Volume of polymer gels coupled to deformation." *Soft Matter* 8(31): 8017-8029.
- Urayama, K., et al. (2008). "Markedly compressible behaviors of gellan hydrogels in a constrained geometry at ultraslow strain rates." *Polymer* 49(15): 3295-3300.
- Vervoort, S., et al. (2005). "Solvent release from highly swollen gels under compression." *Polymer* 46(1): 121-127.
- Wang, H., et al. (2018). "Highly stable perovskite nanogels as inks for multicolor luminescent authentication applications." *Journal of Materials Chemistry C* 6(43): 11569-11574.
- Zanina, A. and T. Budtova (2002). "Hydrogel under shear: a rheo-optical study of the particle deformation and solvent release." *Macromolecules* 35(5): 1973-1975.

- Zhang, H., et al. (2010). "Using screening test results to predict the effective viscosity of swollen superabsorbent polymer particles extrusion through an open fracture." *Industrial & engineering chemistry research* 49(23): 12284-12293.
- Zhang, Y., et al. (2017). "A Variable Mass Meso-Model for the Mechanical and Water-Expelled Behaviors of PVA Hydrogel in Compression." *International Journal of Applied Mechanics* 9(03): 1750044.

VITA

Xinrui Zhao received his Bachelor of Science degree in Petroleum Engineering from Missouri University of Science and Technology in May 2017. He started his master degree at Petroleum Engineering department of Missouri University of Science and Technology from August, 2017. He joined Dr. Baojun Bai's research group from August, 2017 and worked as a research assistant. In May, 2019, he received his degree of Master of Science in Petroleum Engineering from Missouri University of Science and Technology.